agronomy

MDPI

Article

Local Factors Impact Accuracy of Garlic Tissue Test Diagnosis

Leandro Hahn [1], Léon-Étienne Parent [2], Anderson Luiz Feltrim [1], Danilo Eduardo Rozane [3], Marcos Matos Ender [4], Adriele Tassinari [5], Amanda Veridiana Krug [5], Álvaro Luís Pasquetti Berghetti [6,*] and Gustavo Brunetto [5]

1 Caçador Experimental Station, Santa Catarina State Agricultural Research and Rural Extension Agency, (EPAGRI), Caçador 89501-032, SC, Brazil
2 Department of Soils and Agrifood Engineering, Université Laval, Québec, QC G1V 0A6, Canada
3 Agronomy Department, São Paulo State University "Júlio Mesquita Filho", Registro 11900-000, SP, Brazil
4 Agronomy Department, University of Alto Vale do Rio do Peixe (UNIARP), Caçador 89500-000, SC, Brazil
5 Soil Science Department, Federal University of Santa Maria (UFSM), Santa Maria 97105-900, RS, Brazil
6 Forest Science Department, Federal University of Paraná (UFPR), Santa Maria 97105-900, RS, Brazil
* Correspondence: alvaro.berghetti@gmail.com

Abstract: The low productivity of garlic in Brazil requires more efficient nutritional management. For this, environmental and fertilization-related factors must be adjusted to a set of local conditions. Our objective was to provide an accurate diagnosis of the nutrient status of garlic crops in southern Brazil. The dataset comprised 1024 observations, 962 as field tests conducted during the 2015–2017 period to train the model, and 61 field observations collected during the 2018–2019 period to validate the model. Machine learning models (MLM) related garlic yield to managerial, edaphic, plant, and climatic features. Compositional data analysis (CoDa) methods allowed classification of nutrients in the order of limitation to yield where MLM detected nutrient imbalance. Tissue analysis alone returned an accuracy of 0.750 in regression and 0.891 in classification about the yield cutoff of 11 ton ha^{-1}. Adding all features documented in the dataset, accuracy reached 0.855 in regression and 0.912 in classification. Local diagnosis based on MLM and CoDa and accounting for local features differed from regional diagnosis across features. Local nutrient diagnosis may differ from regional diagnosis because several yield-impacting factors are taken into account and benchmark compositions are representative of local conditions.

Keywords: Adaboost; *Allium sativum*; compositional distance; growth-limiting factors; machine learning; perturbation vector; random forest

Citation: Hahn, L.; Parent, L.-É.; Feltrim, A.L.; Rozane, D.E.; Ender, M.M.; Tassinari, A.; Krug, A.V.; Berghetti, Á.L.P.; Brunetto, G. Local Factors Impact Accuracy of Garlic Tissue Test Diagnosis. *Agronomy* **2022**, *12*, 2714. https://doi.org/10.3390/agronomy12112714

Academic Editor: Paul Kwan

Received: 5 September 2022
Accepted: 18 October 2022
Published: 1 November 2022

1. Introduction

Garlic (*Allium sativum* L.) yield averaged 11 Mg ha^{-1} in Brazil, compared with 17 Mg ha^{-1} worldwide [1].Garlic yield and quality depend mainly on temperature, precipitation, and photoperiod, hence local factors [2]. Associated with this, climate change that is causing the irregular distribution of rainfall can be a limiting factor for garlic production [3,4]. However, the Brazilian yield gap could be filled through genetics [5–7], pest management [8], irrigation [9], and fertilization [1,10]. Several garlic cultivars of high commercial value [6,11] are grown under widely different local conditions in the Brazilian states of Minas Gerais, Goiás, Santa Catarina, and Rio Grande do Sul.

Fertilization programs can be guided by soil and plant testing methods [12,13]. Compared with soil tests, tissue tests are generally more closely related to crop performance because the plant can integrate many site-specific abiotic factors [14,15] and nutrient interactions [16]. Cunha et al., 2016, elaborated regional nutrient standards for the noble garlic cultivar "Ito" using a dataset of 142 observational data from Minas Gerais, Brazil. However, a larger and more diversified dataset is required to diagnose nutrient problems across various growing conditions in the southern Brazilian states.

To address nutrient interactions, tissue test interpretation was thought to be universal using pairwise ratios [17], but the assumption proved to be wrong at the local scale [18–20]. Optimum tissue nutrient concentration ranges may also vary with early biomass production due to differential growth rates and environmental conditions [21]. The "dilution effect" and its inverse, the "concentration effect", occur when the concentration of an element decreases or increases in plant tissue through time due to nutrient additions and changing seasonal environmental conditions that impact plant growth rate and the production of biomass [22]. Hence, key growing factors should be considered to predict yield from tissue analysis. This is especially true for fast-growing annual crops such as garlic.

Factor-specific nutrient diagnosis of agroecosystems could be conducted following Alexander von Humboldt's principles of biogeography where facts and local knowledge are assembled and processed by machine learning methods such as decision trees to reach a comprehensive understanding of living systems [23]. On the other hand, the properties of living systems are often reported in terms of concentrations or percentages. Analyzing raw compositions numerically is a very difficult and time-consuming task [24]. Compositional data analysis (CoDa) has been developed to address the limitation related to dilution of concentration among D components that are constrained to the unit sum and provide D-1 degrees of freedom when conducting statistical analyses [25].

Combining machine learning and compositional data analysis methods sequentially proved to be accurate for yield predictions and the detection of nutrient problems at the local scale [18,19,26–29]. Machine learning methods can predict crop yield in regression or classification modes. The classification mode allows growers to select realistic site-specific yield targets and provides risk analysis as the probability to exceed a target yield. For nutritionally imbalanced plants, nutrients can be ordered thereafter according to their limitation to yield using tools of compositional data analysis. The following hypotheses were tested: (1) optimum nutrient combinations of garlic tissues are factor specific, and (2) machine learning and compositional data analysis methods predict garlic yields and nutrient limitations differently using local conditions vs. regional averages. Our objective was to provide an accurate diagnosis of the nutrient status of garlic crops in southern Brazil.

2. Materials and Methods

2.1. Experimental Area Description

The garlic dataset was collected in Fraiburgo (−27.04 S, −50.83 W), Santa Catarina state, Brazil. The dataset comprised 962 field tests conducted during the 2015–2017 period, and 61 field observations collected during the 2018–2019 period, totaling 1024 observations (Table S1). The climate of the region is warm temperate (Cfb) according to the Köppen's classification system. The mean temperature of the region is 16.4 °C and the mean annual rainfall is 1711 mm [30]. The landscape is moderately plain to slightly undulated. Soils are of clayey texture and are classified as Typic Hapludox [31].

Plots were 5 m in length, arranged in beds made of three double rows, with a spacing of 10 cm between rows and 35 cm between double rows and sprinkler irrigated [10]. The beds were 1.7 m wide center-to-center. Virus-free cloves were vernalized at 2–5 °C for 20–30 d before planting at 45 seed cloves m^{-2}. Noble cultivars were "Chonan", "Ito", "Quitéria", "Roxo Caxiense", and "São Valentin" [7]. Cloves were planted between 7 May and 26 July, and harvested between 3 November and 5 December. The length of the growing seasons varied between 102 and 162 days, depending on the cultivar. Cultural practices and pest management strategies were those currently used in the region.

There were 34 fertilizer trials in 2015 (5 N, 14 P, and 15 K), 28 trials in 2016 (6 N, 10 P, and 12 K), and four trials in 2017 (4 N). The plants received five N doses between 0 and 400 kg N ha^{-1} (as ammonium nitrate) in three equal top-dress applications up to 133 kg N ha^{-1} at planting, 30 d after planting, and 10–15 days after bulb differentiation. Where N was varied, the P and K treatments were applied at rates of 175 kg P_2O_5 ha^{-1} (as triple superphosphate) and 333 kg K_2O ha^{-1} (as potassium chloride). The P_2O_5 and K_2O were applied to the soil surface and incorporated into the 0–20 cm layer using a rotary tiller

before garlic was planted. Where P_2O_5 and K_2O were varied, the N was applied at a rate of 300 kg N ha^{-1} in three equal doses of 100 kg N ha^{-1} each, top-dressed at planting, 30 d after planting and 10–15 days after bulb differentiation. Growers' treatments were applied on one farm in 2018 and on two farms in 2019.

2.2. Soil and Tissue Analyses

Soils were sampled (0–20 cm) 25–30 days after planting. Eight sub-samples were collected per plot. Soils were air-dried and ground to less than 2 mm before conducting chemical analyses as follows [32]: water pH = 5.9 (ratio 1:1), clay by sedimentation, Mehlich-1 extraction for P and K, and EDTA extraction for Cu [33]. Elements were quantified by plasma emission spectroscopy (ICP-OES) and sulfur by turbidimetry. Cation exchange capacity was approximated as the sum of exchangeable cations and total acidity (SMP buffer pH). Total carbon was quantified by dichromate oxidation (Walkley–Black method) and then multiplied by 1.724 to obtain the organic matter content [33].

Ten young (4th fully expanded) leaves were collected in each plot at the beginning of plant differentiation into bulbs [2], averaging 93 days after planting and 12 days before the last N application. Tissue samples were composited for chemical analysis. The leaves were gently washed under distilled water, dried at 65 ± 5 °C, then ground to less than 1 mm using a Wiley mill [34]. Total N was determined by steam distillation. Tissue samples were digested in a mixture of nitric and perchloric acids, in the proportion 2:1 (v/v) [12] then analyzed by colorimetry for P [35] and B [36], flame photometry for K, turbidimetry for S, and atomic absorption spectrophotometry for Ca, Mg, Cu, Fe, Mn, and Zn [32].

Bulbs were harvested in 1 m length rows made of three double plant lines per plot [10]. The bulbs were weighed after natural drying in a warehouse for 40 d. Marketable bulbs included #2 (<32 mm), #3 (32–37 mm), #4 (37–42 mm), #5 (42–47 mm), #6 (47–56 mm), and #7 (>56 mm) bulb categories [37]. Bulbs showing secondary growth or damage were classified as non-marketable.

2.3. Climatic Indices

Daily precipitations as well as minimum and maximum daily temperatures between plantation and tissue sampling dates were obtained from EPAGRI meteorological station up to 30 km away from the planting area. [38]. The photoperiod was reflected by the planting date. Temperature data were synthesized as cumulated degree days with a base temperature of 5 °C for cold crops [39]. Rainfall was cumulated between planting and tissue sampling dates. Rainfall distribution was assessed using the Shannon diversity index (SDI) as follows [40]:

$$\mathrm{SDI} = \frac{-\sum_{i=1}^{n} p_i \times ln(p_i)}{ln(p_i)} \quad (1)$$

where: p_i is the fraction of daily rainfall relative to total rainfall during the growing period and n is the length of the growing season; SDI = 1 indicates uniformly distributed rainfall (equal daily amount of rainfall over the selected period); and SDI = 0 indicates uneven rainfall (total rainfall concentrated in 1 d). Where $p_i = 0$, $p_i \times ln(p_i) = 0$. Crops were irrigated until the soil moisture reached field capacity, but the frequency and amount of water applied by the irrigation event were not recorded.

2.4. Numerical Analyses

Machine learning models related the marketable yield to features using the Orange data mining software v. 3.23 [41]. We compared random forest and Adaboost. Models were run in regression and classification modes. In classification mode, true negative specimens (high-yielding, nutritionally balanced) used as benchmark compositions were set apart in the confusion matrix (Figure 1). The models were trained using the 2015–2017 data (64 fertilizer trials) in cross-validation (k = 10, stratified by category). In brief, ten percent of the data were thus selected randomly ten times to train the model. The remaining data were used each time to validate the model. Model accuracy was the average of the ten

runs. Model accuracy may vary slightly by reloading the file and rerunning the models because data selection changes at each run. The impact of features on model accuracy was measured by sequentially adding features. Models were tested in prediction mode using the 2018–2019 data.

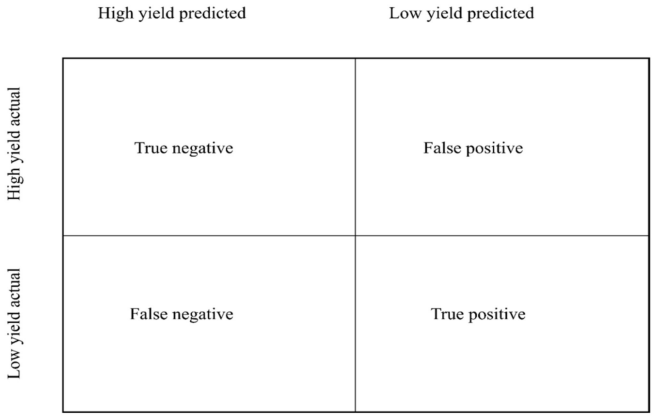

Figure 1. Specimen classification in the confusion matrix into true negative (TN), true positive (TP), false positive (FP), and false negative (FN).

Regional standards were computed as centered log ratio means and standard deviations of compositions across true negative specimens as follows [19,41,42]:

$$clr_{x_i} = ln(x_i/G) \tag{2}$$

where: *clr* is the centered log ratio of component x_i and G is the geometric mean across components x_i including the filling value computed by the difference between the measurement unit and the sum of quantified components.

The regional diagnosis was conducted as follows:

$$Index_{x_i} = \frac{\left(clr_{x_i} - \overline{clr^*_{x_i}}\right)}{SD^*_{x_i}} \tag{3}$$

where: $\overline{clr^*_{x_i}}$ and $SD^*_{x_i}$ are the mean and standard deviation for component x_i of the subpopulation of true negative specimens. Nutrients were classified in the order of limitation to yield from the most negative to the most positive $Index_{x_i}$ values.

Local diagnoses were conducted by computing the Euclidean distance from the diagnosed composition to select close compositional neighbors, as follows [19,20,27]:

$$\varepsilon = \sqrt{\sum_{i=i}^{D}\left(clr_{x_i} - clr_{y_i}\right)^2} \tag{4}$$

where: ε is the Euclidean distance between the diagnosed composition, x and successful compositions y, i.e., the Euclidian distance is computed across *clr* differences. The Euclidean distance indicates the closest true negative specimens to be used to guide the rebalancing of the nutrients in the diagnosed specimens.

Nutrients in the diagnosed specimens were classified in the order of limitation to yield from the most negative to the most positive values against the benchmark composition of the closest true negative specimens using the perturbation vector standardized as follows:

$$p = X \ominus Y = \left\{\frac{N}{N^*}, \frac{P}{P^*}, \ldots, \frac{F_v}{F_v^*}\right\} \tag{5}$$

where: * indicated components of the reference benchmark composition among high-yielding and nutritionally balanced true negative specimens under otherwise comparable local conditions. The perturbation vector (calculated based on the nutritional ratio, a successful and a defective composition) was balanced around zero as follows:

$$p = X \ominus Y = \left\{ \frac{N}{N^*} - 1, \frac{P}{P^* - 1}, \ldots, \frac{F_v}{F_v^*} - 1 \right\} \quad (6)$$

The perturbation vector resembles the deviation from optimum percentage [42] with the selection of the benchmark composition based on the Euclidean distance.

3. Results

3.1. Model Accuracy

Machine learning methods can predict absolute yield from a regression equation or can provide risk analysis as the probability to reach yields higher than the target yield. The training dataset (the 914 observations collected in 2015–2017) was evaluated in regression mode using Adaboost and in classification mode using random forest. These machine learning methods showed the highest performance among other machine learning methods (data not shown). Results are presented in Figure 2 and Table 1. Model accuracy increased as learners were more informed about features (Table 2).

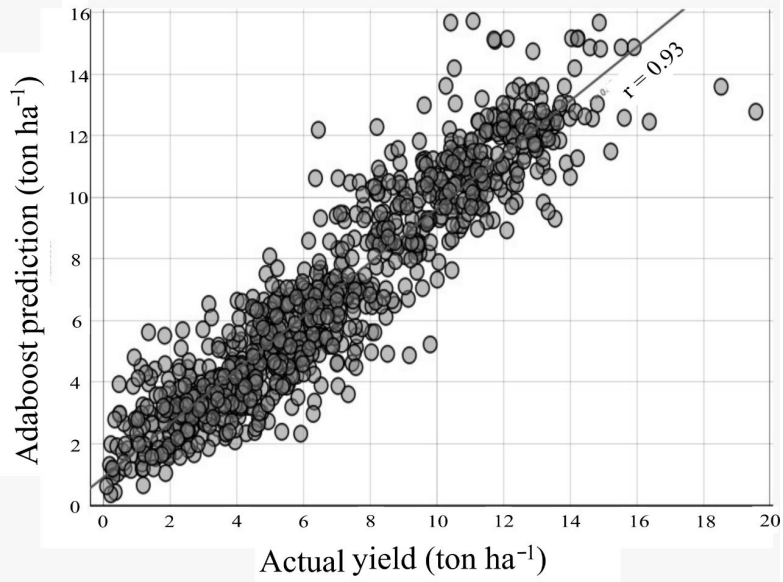

Figure 2. Adaboost regression model relating marketable yield to genetic (cultivar), managerial (plantation date, fertilization at planting, and 30 d after planting), tissue test, soil test, and climatic features.

Table 1. Random forest yield classification of the training garlic calibration dataset (2015–2017) made of 914 observations, showing an accuracy of 0.912, i.e., (135 + 699)/914.

Yield Classification	Predicted Yield	
Actual yield	High	Low
High	135 TN	40 FP
Low	40 FN	699 TP

TN = true negative; FN = false negative; FP = false positive; and TP = true positive.

Table 2. Accuracy of the Adaboost in regression mode and random forest in classification mode for the garlic training dataset collected in 2015–2017.

Combination of Factors	Regression R^2	Classification Accuracy
Tissue analysis	0.750	0.891
Tissue analysis, cultivar	0.789	0.886
Tissue analysis, cultivar, preceding crop	0.791	0.894
Tissue analysis, cultivar, preceding crop, fertilization	0.820	0.898
Tissue analysis, cultivar, preceding crop, fertilization, plantation date	0.839	0.891
Tissue analysis, cultivar, preceding crop, fertilization, plantation date, climatic indices	0.840	0.907
Tissue analysis, cultivar, preceding crop, fertilization, plantation date, climatic indices, soil test	0.855	0.912

Accuracy of the random forest classification model was 0.912 with 135 true negative specimens at yield cutoff set at Brazilian yield average of 11 ton ha^{-1} (Table 2). At yield cutoff of 8 ton ha^{-1}, classification accuracy reached the maximum value at 0.955 with 345 true negative specimens. There were significant differences between regional nutrient standards for yield cutoffs of 8 ton ha^{-1} or 11 ton ha^{-1} (Table 3). Because yield cutoff is often arbitrarily selected but impacts on the number of true negative specimens, regional nutrient diagnosis should be interpreted in relation to yield target and local conditions.

Table 3. Regional centered log ratio means and standard deviation computed across *n* true negative specimens at garlic yield cutoffs of 8 Mg or 11 Mg marketable yield ha^{-1}, respectively.

Nutrient	8 Mg ha^{-1}		11 Mg ha^{-1}		*t*-Test Probability
	Mean	SD	Mean	SD	
N	3.430	0.157	3.403	0.166	0.112 ^{ns}
P	1.365	0.209	1.317	0.167	0.011 *
K	3.255	0.235	3.364	0.193	0.000 **
Ca	1.463	0.345	1.642	0.242	0.000 **
Mg	0.679	0.229	0.532	0.123	0.000 **
S	1.843	0.423	1.938	0.379	0.019 *
Fe	−3.786	0.393	−3.814	0.423	0.509 ^{ns}
Mn	−3.070	0.505	−3.062	0.415	0.861
Zn	−3.583	0.481	−3.725	0.395	0.001 **
Cu	−3.918	0.336	−3.877	0.280	0.186 ^{ns}
B	−4.516	0.828	−4.495	1.012	0.836 ^{ns}
F_v	6.838	0.191	6.779	0.186	0.002 **
Number	*n* = 344		*n* = 128		-

Mean = n; SD = standard deviations; Fv = filling value. ^{ns},*, **: nonsignificant and significant at $p < 0.05$.

3.2. Random Forest Yield Prediction for Observational Data in 2018–2019

Climatic indices in 2018 and 2019 differed markedly from those recorded in 2015–2017 (Table 4). From planting to the tissue sampling date, cumulated rainfall was low and rainfall distribution was uneven in 2019 while conditions in 2018 were closer to those observed during the 2015–2017 period. Tissue compositions in 2018 and 2019 often differed from those recorded as true negative specimens during 2015–2017 period. Despite contrasting features between experimental (2015–2017) and observational (2018–2019) datasets, yield classification was predicted tentatively by the random forest classification model setting yield cutoff at the Brazilian average of 11 ton ha^{-1}. This emphasizes the need for larger and more diversified training datasets in addition to greater control of variables associated with management such as irrigation.

Table 4. Range of values for features to predict yields observed in 2018–2019 from the experimental dataset (2015–2017).

Feature ‡	Site 2018	Site 2019 A	Site 2019 B	True Negative Specimens
N	20.0–33.3	33.6–39.2	19.6–36.4	23.1–45.5
P	4.8–6.6	4.5–5.0	3.6–6.9	2.1–5.8
K	28.4–81.2	41.9–52.0	10.8–29.9	12.7–54.5
Ca	15.7–50.4	7.1–9.7	3.4–5.1	0.9–9.8
Mg	2.9–7.9	3.9–5.1	1.7–8.5	0.8–2.5
S	6.5–9.4	3.9–5.8	3.3–7.0	3.5–14.5
B	54–86	18–23	26–40	0.9–44
Fe	32–197	98–339	28–137	13–515
Mn	59–176	35–92	19–39	11–115
Zn	43–107	26–38	22–57	10–154
Cu	16–54	4–8	7–56	3–219
Degree-days (>5 °C)	461	582	347	297–421
Rainfall (mm)	172	41	35	104–241
SDI	0.57	0.10	0.04	0.54–0.64

‡ Macronutrients expressed in g kg^{-1}; micronutrients expressed in mg kg^{-1}. From plantation to tissue sampling dates. SDI = Shannon diversity index.

Where risk analysis showed more than 50% probability to reach a yield above the target, the predicted yield was declared "high". While 52 of the 61 specimens yielded more than 11 ton ha^{-1} during the 2018–2019 period, seven specimens were classified as true negative (high-yielding and nutritionally balanced) and 45 specimens as false positive (high-yielding and nutritionally imbalanced). The remaining nine specimens were classified as true positive specimens (low-yielding and nutritionally imbalanced).

The 28 specimens in 2018 showed 100% probability of being classified as false positive, indicating luxury consumption, suboptimum concentration, or nutrient contamination, therefore, unwise use of fertilizers. The nine specimens at site A in 2019 were low-yielding and imbalanced, showing less than 16% probability to be classified as true negative, therefore, the fertilization regime appeared to be inappropriate. At site B in 2019 where yield always exceeded 11 ton ha^{-1}, there were 4 true negative and 20 false positive specimens. The classification of median values across observational specimens indicated false positive specimens in 2018, true positive specimens at site A in 2019, and false positive specimens at site B in 2019.

3.3. The False Positive Specimens at Site in 2018

The yield of the diagnosed specimen was 15.5 ton ha^{-1} compared with 11.0–11.2 ton Mg ha^{-1} for the closest reference specimens (Table 5). There was a large difference between regional and local diagnoses (Figure 3). Regional diagnosis indicated an apparent shortage of N, P, and K despite the high yield. Local diagnosis indicated an excess across nutrients. Compared with its closest compositional neighbor, the grower had fair control of N fertilization but failed to adjust other nutrients to crop needs. There were excessive accumulations of P and K in the soil. There was a large potential for economic and environmental gains by reducing fertilization.

Table 5. Difference in yield and soil and tissue compositions in the diagnosed specimen in 2018 and its closest nutritionally balanced neighbors yielding more than 11 Mg ha^{-1}.

Variable	Unit	Diagnosed	First Nearest	Second Nearest	Third Nearest
Yield	Mg ha^{-1}	15.5	11.2	11.0	11.1
		Tissue			
N	g kg^{-1}	29.5	30.0	28.9	28.0
P	g kg^{-1}	5.9	4.1	3.2	2.8
K	g kg^{-1}	35.0	33.3	30.8	32.0
Ca	g kg^{-1}	21.0	5.1	4.4	4.8
Mg	g kg^{-1}	3.5	1.8	1.9	1.7
S	g kg^{-1}	7.6	5.8	4.7	8.3
B	mg kg^{-1}	64	33	31	28
Fe	mg kg^{-1}	55	42	41	30
Mn	mg kg^{-1}	97	73	84	22
Zn	mg kg^{-1}	62	32	31	28
Cu	mg kg^{-1}	28	29	4	6
		Soil			
pH_{water}	-	6.4	6.3	6.0	6.1
Clay	%	40	61	61	49
OM	%	5.7	3.6	3.8	3.2
P	mg dm^{-3}	131.2	8.6	8.9	19.4
K	mg dm^{-3}	400	298.1	552	132
Ca	$cmol_c$ dm^{-3}	12.4	8.5	7.1	9.4
Mg	$cmol_c$ dm^{-3}	4.9	2.3	3.1	3.7
		Treatment			
N	kg N ha^{-1}	160	400	400	400
P	kg P_2O_5 ha^{-1}	680	0	400	100
K	kg K_2O ha^{-1}	457	400	500	400

Figure 3. Local diagnosis of a high-yielding false positive specimen against the nearest successful neighbor before and after removing cationic micronutrients. There is a relative excess of Ca, B, S, Mg, and P attributable to luxury consumption. Fv = filling value. Negative differences between defective and successful specimens indicate relative shortage. Positive differences indicate relative excess.

3.4. The True Positive Specimens at Site A in 2019

The nearest compositional neighbor showed a marketable yield of 13.9 ton ha^{-1} compared with 9.7 ton ha^{-1} for the diagnosed specimen. Soil tests of P, K, Ca, and Mg at site A in 2019 for the reference specimen as well as other features are reported in Table 6. Organic matter content was 4.5% for the diagnosed site and 3.8% in the reference specimen, indicating a possible need for site-specific management of nitrogen [43]. The grower already took action to reduce N fertilization from 400 to 130 kg total N ha^{-1}. Both local and regional diagnoses indicated tissue P, K, Ca, and Mg excess compared with the three closest tissue compositional neighbors (Table 6). Factor-specific diagnosis at the local scale indicated

relative excess of macronutrients, as well as Zn and Cu (Figure 4). However, the Zn and Cu levels must vary with the time and rate of fungicide applications. Compared with its closest composition neighbor, the producer reduced N application.

Table 6. Difference in yield and soil and tissue compositions in the diagnosed specimen at site A in 2019 and its closest nutritionally balanced neighbors yielding more than 11 ton ha^{-1}.

Variable	Unit	Diagnosed	First Nearest	Second Nearest	Third Nearest
Yield	ton ha^{-1}	9.7	13.9	11.0	11.4
		Tissue			
N	g kg^{-1}	39.2	26.0	28.9	28.8
P	g kg^{-1}	4.8	2.9	3.2	2.6
K	g kg^{-1}	48.7	28.1	30.8	25.1
Ca	g kg^{-1}	8.4	4.1	4.4	3.6
Mg	g kg^{-1}	4.5	2.0	1.9	1.4
S	g kg^{-1}	5.1	4.5	4.7	7.9
B	mg kg^{-1}	202	272	315	255
Fe	mg kg^{-1}	1264	857	410	420
Mn	mg kg^{-1}	478	550	840	216
Zn	mg kg^{-1}	288	185	308	263
Cu	mg kg^{-1}	63	30	43	38
pH_{water}		6.0	6.0	6.0	6.1
Clay	%	39	61	61	49
OM	%	4.5	3.8	3.8	3.2
P	mg dm^{-3}	47.5	31.7	8.9	15.2
K	mg dm^{-3}	296	112.3	552	132
Ca	$cmol_c$ dm^{-3}	15.3	7.1	7.1	9.4
Mg	$cmol_c$ dm^{-3}	5.0	3.1	3.1	3.7
		Treatment			
N	kg N ha^{-1}	130	300	300	300
P	kg P_2O_5 ha^{-1}	300	800	400	0
K	kg K_2O ha^{-1}	150	400	500	400

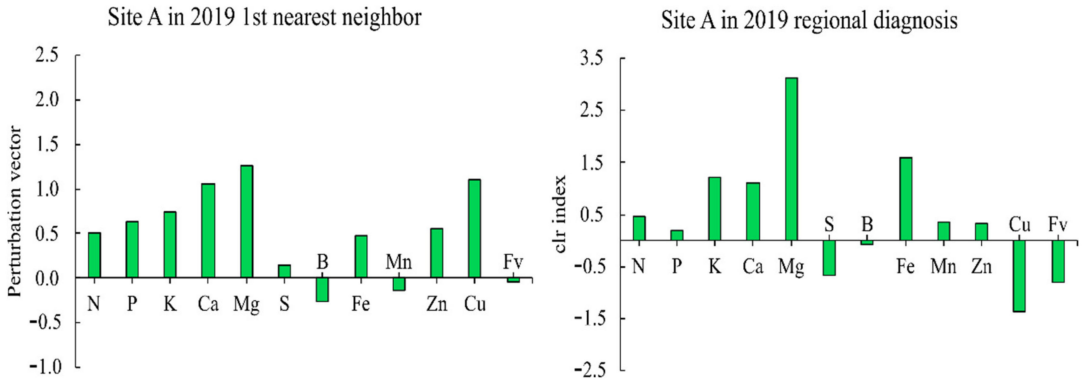

Figure 4. Nutrient diagnosis at local scale at site A in 2019 slightly differed from nutrient diagnosis at the regional scale. The difference in Cu diagnosis is attributable to the time and rate of fungicide applications. Fv = filling value. Negative differences between defective and successful specimens indicate relative shortage. Positive differences indicate relative excess.

4. Discussion

4.1. Factor-Specific Optimum Nutrient Levels

At optimum yield, N requirements generally depend on crop yield and tissue N content. K bioavailability depends on the clay type, and P bioavailability depends on the plant rooting pattern and competition, root hairs, mycorrhizal and other microbial

associations, and also soil P sorption capacity and soil chemicals, such as pH, or physical barriers [44,45]. Considering those limitations, nutrient budgets were elaborated using a sequence of equations and plant- and soil-specific coefficients [34]. Although partially applied to garlic nutrition [1], such an approach could be inaccurate if not validated by fertilizer trials as was the case for tomato (*Solanum lycopersicum* L.) in São Paulo state, Brazil [46]. Alternatively, tissue testing can integrate several growth-impacting factors [15]. However, there are currently no reliable guidelines for tissue testing that address the nutrient management of garlic at the local scale.

Seasonal variations in tissue nutrient concentrations depend on biomass accumulation at a given developmental stage under specific growing conditions [21]. Fast-growing crops take up more N than slow-growing crops during their vegetative phase when most decisions on fertilization are made [21]. The N, P, and K concentration and dilution phenomena show allometric relationships with plant biomass [21,47]. Indeed, N, P, and K concentrations in plants tend to decrease simultaneously through time [17]. Because nutrient allocation patterns in response to the abiotic or biotic environments are plastic [48,49], tissue analytical results should not be interpreted in isolation. We showed that informing the machine learning model with an increasing number of yield-impacting abiotic and biotic features can increase model accuracy. Tissue sampling position, plant developmental stage, row spacing, plant population, fertilizer source, placement, rate and timing, and pest control were assumed to be similar between sites as current practices in the region.

4.2. Prediction of Garlic Yields and Nutrient Limitations

Machine learning methods can address the specificity of factor combinations impacting crop nutrition and yield. A minimum dataset easy to acquire by garlic growers may include cultivar, the preceding crop, planting date, tissue test, soil test, fertilization, and climatic factors impacting plant growth during the vegetative phase up to tissue sampling. Because late-season tissue nutrient diagnosis is an ex ante approach to predict final yield with uncertainty, growers may prefer the classification mode to provide the probability of reaching the selected target yield.

Growers often report differential growth patterns for plants growing on the same field without any nutrient deficiency symptoms. Those plants are typically false negative specimens. In this case, the abnormally low growth pattern is attributable to stress rather than mineral nutrition, caused by factors such as pest damage or adverse soil physical conditions. Plants may also be true positive specimens, high-yielding but nutritionally mismanaged [20]. The advantages of local over regional diagnoses are that (1) several climatic, edaphic, and managerial growth factors can be trustfully assumed to be equal for the same ecological neighborhood, and (2) yield target is realistic for that neighborhood. Another advantage of local diagnosis is to avoid over-representation of some ecologically uniform groups of true negative specimens that may not be representative of local conditions but are still used to compute nutrient standards at the regional scale. The focus is to consider local conditions comparable to those of the diagnosed specimen to run the diagnosis. The authors of [26,27] thus developed the concept of "enchanting islands" as successful environments where controllable factors can be optimized. Leitzke Betemps et al., (2020) also called such benchmark locations "Humboldtian loci" or "Ilhas Encantadas" in Portuguese. That is, mathematical simulations for nutritional diagnoses in geographically close locations, taking into account areas of adequate productivity (Humboldtian loci) as a reference, which are surrounded by areas with low productivity. The objective was to address controllable factors in such a way to re-establish nutrient balance or heal physically unhealthy soils in an economically and environmentally viable fashion.

On the other hand, nutrient imbalance to be tackled should not be diagnosed by examining nutrients separately. Any nutrient level is impacted by the level of other nutrients under Liebscher's law of the optimum [50]. This phenomenon has been reported as "nutrient interactions" [16], "dual or pairwise interactions" [51], "multinutrient interactions" [52], "nutrient crosstalks" [53] or, in CoDa terms, "resonance within the simplex" [24]. Vahl de

Paula et al., (2020) viewed soil and tissue compositions as unique combinations of nutrients that differ from "Frankenstein-built" regional standards, that is, constructed from data that do not interact with each other and do not provide useful information for nutritional diagnosis, averaged across contrasting growth-impacting factors.

The geometry of log ratio transformations facilitates the search for nutritionally close compositional neighbors growing under comparable conditions. Where nutrient imbalance is detected by the machine learning model, nutrients can be classified in a relative order of limitation to yield to assist making wise decisions on how to adjust fertilization. The perturbation vector [24] used to classify nutrients resembles the deviation from optimum percentage [42], but the benchmark compositions can be tied to attainable yields among true negative specimens located in nearby "Ilhas Encantadas".

4.3. Need for Large and Diversified Datasets

Beaufils (1971) documented several features impacting yield parameters as follows: (1) vegetative conditions such as appearance (normal or abnormal plants or stands as luxurious, luxurious to medium, medium, medium to poor, or poor), tissue sampling position, plant age measured by the difference between plantation and tissue sampling dates, hour of tissue sampling, leaf color, plant height, visual symptoms, disease, and insect infestation; (2) weather conditions such as rainfall, temperature, wind, and light intensity; (3) cultivation practices such as cultivar, date of planting, row spacing, plant population, fertilizer source, placement, rate and timing, pesticides, and site history; (4) soil chemical, physical, and mechanical quality; and (5) leaf analysis. Biological soil quality based on tools of metagenomics is also gaining acceptance [54]. While the test dataset in 2018–2019 showed features that differed from the training dataset, yield class predictions from extrapolated features must be interpreted with caution. Nutrient diagnosis using the random forest classification model also depended on the selected cutoff yield and the number of factors documented in the dataset.

Yield of garlic could be predicted accurately using a dataset easy to acquire by the grower, including cultivar, fertilization, tissue analysis, soil analysis, and the preceding crop and climatic conditions between plantation and tissue sampling dates. Compositional log ratio methods provided an order of nutrient limitations to yield useful benefits to customize fertilizer recommendations at the local scale. Nevertheless, large and diversified datasets should thus be documented by experimental and observational data in collaboration with stakeholders.

5. Conclusions

Optimum nutrient combinations to reach high-yield level under specific local conditions were shown to be factor specific. Tissue analysis alone returned an accuracy of 0.750 in regression mode, and of 0.891 in classification mode using a yield cutoff of 11 ton ha^{-1}. However, accuracy reached 0.855 in regression mode and 0.912 in classification mode where models included all factors documented in the dataset. Because biomass production and other factors must impact tissue compositions, it is recommended to include all factors that are easy to acquire by the grower to run nutrient diagnosis of garlic crops.

Garlic can grow successfully under various combinations of nutrients subjected to a number of edaphic and managerial local factors. Local nutrient diagnosis may differ from regional diagnosis because several yield-impacting factors are taken into account and benchmark compositions are representative of local conditions. As datasets become larger in size and diversity, local diagnosis will provide effective and economical use of nutrient resources to reach a high yield of garlic. Increased economic and environmental concerns should cause many growers to re-assess nutrient management strategies so that inputs and costs are minimized while yield expectations are met. Collaboration among stakeholders is required to tackle the numerous factor combinations of yield-impacting factors and to address knowledge gaps to be filled by additional fertilizer trials.

Supplementary Materials: The following supporting information can be downloaded at: https://www.mdpi.com/article/10.3390/agronomy12112714/s1, Table S1: Dataset of garlic production, climate and soil and tissue analysis.

Author Contributions: Conceptualization: L.H., A.L.F. and D.E.R.; data curation: L.-É.P., A.L.F. and M.M.E.; formal analysis: D.E.R.; funding acquisition: L.H.; investigation: L.H., A.L.F. and M.M.E.; methodology: L.H., A.L.F., D.E.R. and G.B.; project administration: L.H.; resources: L.H.; software: L.-É.P.; supervision: L.H. and G.B.; writing—original draft preparation: L.-É.P., A.L.F., M.M.E. and Á.L.P.B.; writing—review and editing: Á.L.P.B., A.T., A.V.K. and G.B. All authors have read and agreed to the published version of the manuscript.

Funding: This research was funded by Santa Catarina State Agricultural Research and Rural Extension Agency, EPAGRI (Seplan N. 6312106) and Alto Vale do Rio do Peixe University (edital FAP 001/2015 e 001/2016) and the Natural Sciences and Engineering Research Council of Canada (NSERC-2254).

Institutional Review Board Statement: Not applicable.

Informed Consent Statement: Not applicable.

Data Availability Statement: Not applicable.

Acknowledgments: The authors are thankful to the Santa Catarina State Agricultural Research and Rural Extension Agency, EPAGRI (Seplan N. 6312106), and Alto Vale do Rio do Peixe University (edital FAP 001/2015 e 001/2016), and the Natural Sciences and Engineering Research Council of Canada (NSERC-2254) for the financial resources provided to this study. The authors would also like to thank all staff of the Caçador Experimental Station, EPAGRI, for the maintenance and data collection from the field trial.

Conflicts of Interest: The authors declare no conflict of interest.

References

1. Cunha, M.L.P.; Oliveira, T.F.; Clemente, J.M.; Gentil, T.G.; de Aquino, L.A. Modeling of nutrients demands in garlic crop. *Aust. J. Crop Sci.* **2015**, *9*, 1205–1213. [CrossRef]
2. Cunha, M.L.P.; Aquino, L.A.; Novais, R.F.; Clemente, J.M.; de Aquino, P.M.; Oliveira, T.F. Diagnosis of the Nutritional Status of Garlic Crops. *Rev. Bras. Ciência Solo* **2016**, *40*, e0140771. [CrossRef]
3. Martínez-López, J.A.; López-Urrea, R.; Martínez-Romero, Á.; Pardo, J.J.; Montoya, F.; Domínguez, A. Improving the Sustainability and Profitability of Oat and Garlic Crops in a Mediterranean Agro-Ecosystem under Water-Scarce Conditions. *Agronomy* **2022**, *12*, 1950. [CrossRef]
4. Sánchez-Virosta, Á.; Sánchez-Gómez, D. Thermography as a Tool to Assess Inter-Cultivar Variability in Garlic Performance along Variations of Soil Water Availability. *Remote Sens.* **2020**, *12*, 2990. [CrossRef]
5. Moretti, C.L.; Berg, F.L.N.; Mattos, L.M.; Santos, J.Z.; Saminêz, T.C.O.; Resende, F.V.; Mendonça, J.L.; Lima, D.B. Chemical composition and physical properties of organically grown onions in central Brazil. *Acta Hortic.* **2005**, *688*, 317–321. [CrossRef]
6. Buso, G.S.C.; Paiva, M.R.; Torres, A.C.; Resende, F.V.; Ferreira, M.A.; Buso, J.A.; Dusi, A.N. Genetic diversity studies of Brazilian garlic cultivars and quality control of garlic-clover production. *Genet. Mol. Res.* **2008**, *7*, 534–541. [CrossRef]
7. De Resende, J.T.V.; Morales, R.G.F.; Zanin, D.S.; Resende, F.V.; de Paula, J.T.; Dias, D.M.; Galvão, A.G. Caracterização morfológica, produtividade e rendimento comercial de cultivares de alho. *Hortic. Bras.* **2013**, *31*, 157–162. [CrossRef]
8. Inglis, P.W.; Mello, S.C.M.; Martins, I.; Silva, J.B.T.; Macêdo, K.; Sifuentes, D.N.; Valadares-Inglis, M.C. Trichoderma from Brazilian garlic and onion crop soils and description of two new species: Trichoderma azevedoi and Trichoderma peberdyi. *PLoS ONE* **2020**, *15*, e0228485. [CrossRef]
9. Amorim, J.R.D.A.; Fernandes, P.D.; Gheyi, H.R.; Azevedo, N.C.D. Efeito da salinidade e modo de aplicação da água de irrigação no crescimento e produção de alho. *Pesqui. Agropecuária Bras.* **2002**, *37*, 167–176. [CrossRef]
10. Hahn, L.; Paviani, A.C.; Feltrim, A.L.; Wamser, A.F.; Rozane, D.E.; Reis, A.R. dos Nitrogen doses and nutritional diagnosis of virus-free garlic. *Rev. Bras. Ciência Solo* **2020**, *44*, e0190067. [CrossRef]
11. Hoogerheide, E.S.S.; Azevedo Filho, J.A.; Vencovsky, R.; Zucchi, M.I.; Zago, B.W.; Pinheiro, J.B. Genetic variability of garlic accessions as revealed by agro-morphological traits evaluated under different environments. *Genet. Mol. Res.* **2017**, *16*, gmr16029612. [CrossRef]
12. Jones, J.B.; Case, V.W. Sampling, Handling, and Analyzing Plant Tissue Samples. In *Soil Testing and Plant Analysis*; SSSA Book Series; John Wiley & Sons, Ltd.: Madison, WI, USA, 1990; pp. 549–562. ISBN 9780891188629.
13. Peck, T.R. Soil testing: Past, present and future. *Commun. Soil Sci. Plant Anal.* **1990**, *21*, 1165–1186. [CrossRef]
14. Ruel, J.C.; Horvath, R.; Ung, C.H.; Munson, A. Comparing height growth and biomass production of black spruce trees in logged and burned stands. *For. Ecol. Manag.* **2004**, *193*, 371–384. [CrossRef]

15. Munson, R.D.; Nelson, W.L. Principles and Practices in Plant Analysis. In *Soil Testing and Plant Analysis*; Westerman, R., Ed.; SSSA Book Series; John Wiley & Sons, Ltd.: Madison, WI, USA, 1990; pp. 359–387. ISBN 9780891188629.
16. Wilkinson, S.R.; Grunes, D.L.; Sumner, M.E. Nutrient Interactions in Soil and Plant Nutrition. In *Handbook of Soil Science*; Routledge: Boca Raton, FL, USA, 2000; pp. 89–112.
17. Walworth, J.L.; Sumner, M.E. The Diagnosis and Recommendation Integrated System (DRIS). In *Advances in Soil Science*; Springer: Berlin/Heidelberg, Germany, 1987; pp. 149–188.
18. Leitzke Betemps, D.; Vahl de Paula, B.; Parent, S.-É.; Galarça, S.P.; Mayer, N.A.; Marodin, G.A.B.; Rozane, D.E.; Natale, W.; Melo, G.W.B.; Parent, L.E.; et al. Humboldtian Diagnosis of Peach Tree (Prunus persica) Nutrition Using Machine-Learning and Compositional Methods. *Agronomy* **2020**, *10*, 900. [CrossRef]
19. De Lima Neto, A.J.; de Deus, J.A.L.; Rodrigues Filho, V.A.; Natale, W.; Parent, L.E. Nutrient Diagnosis of Fertigated "Prata" and "Cavendish" Banana (*Musa* spp.) at Plot-Scale. *Plants* **2020**, *9*, 1467. [CrossRef]
20. Vahl de Paula, B.; Squizani Arruda, W.; Etienne Parent, L.; Frank de Araujo, E.; Brunetto, G. Nutrient Diagnosis of Eucalyptus at the Factor-Specific Level Using Machine Learning and Compositional Methods. *Plants* **2020**, *9*, 1049. [CrossRef]
21. Lemaire, G.; Sinclair, T.; Sadras, V.; Bélanger, G. Allometric approach to crop nutrition and implications for crop diagnosis and phenotyping. A review. *Agron. Sustain. Dev.* **2019**, *39*, 27. [CrossRef]
22. Jarrell, W.M.; Beverly, R.B. *The Dilution Effect in Plant Nutrition Studies*; Academic Press: Cambridge, MA, USA, 1981; Volume 34, pp. 197–224. ISBN 0065-2113.
23. Keppel, G.; Kreft, H. Integration and synthesis of quantitative data: Alexander von Humboldt's renewed relevance in modern biogeography and ecology. *Front. Biogeogr.* **2019**, *11*, 1–6. [CrossRef]
24. Aitchison, J. *The Statistical Analysis of Compositional Data*; Chapman & Hall, Ltd.: London, UK, 1986; ISBN 0412280604.
25. Aitchison, J. Principles of Compositional Data Analysis. *Inst. Math. Stat. Lect. Notes Monogr. Ser.* **1994**, *24*, 73–81. [CrossRef]
26. Coulibali, Z.; Cambouris, A.N.; Parent, S.-É. Cultivar-specific nutritional status of potato (*Solanum tuberosum* L.) crops. *PLoS ONE* **2020**, *15*, e0230458. [CrossRef]
27. Parent, S.-É. Why we should use balances and machine learning to diagnose ionomes. *Authorea* **2020**, *1*, 1–13. [CrossRef]
28. Parent, S.-É.; Lafond, J.; Paré, M.C.; Parent, L.E.; Ziadi, N. Conditioning Machine Learning Models to Adjust Lowbush Blueberry Crop Management to the Local Agroecosystem. *Plants* **2020**, *9*, 1401. [CrossRef] [PubMed]
29. Hahn, L.; Parent, L.-É.; Paviani, A.C.; Feltrim, A.L.; Wamser, A.F.; Rozane, D.E.; Ender, M.M.; Grando, D.L.; Moura-Bueno, J.M.; Brunetto, G. Garlic (*Allium sativum*) feature-specific nutrient dosage based on using machine learning models. *PLoS ONE* **2022**, *17*, e0268516. [CrossRef] [PubMed]
30. Alvares, C.A.; Stape, J.L.; Sentelhas, P.C.; Gonçalves, J.L.M.; Sparovek, G. Köppen's climate classification map for Brazil. *Meteorol. Zeitschrift* **2013**, *22*, 711. [CrossRef]
31. United States Department of Agriculture. *Soil Survey Staff Keys to Soil Taxonomy*, 12th ed.; United States Department of Agriculture: Washington, DC, USA, 2014.
32. Tedesco, M.J.; Gianello, C.; Bissani, C.A.; Bohnen, H.; Volkweiss, S.J. *Análise de Solo, Plantas e Outros Materiais*; Universidade Federal do Rio Grande do Sul: Porto Alegre, Brazil, 1995.
33. Da Silva, F.C. *Manual de Análises Químicas de Solos, Plantas e Fertilizantes*; Embrapa Informação Tecnológica: Brasília, Brazil, 2009.
34. Dos Santos, F.C.; Neves, J.C.L.; Novais, R.F.; Alvarez, V.V.H.; Sediyama, C.S. Modelagem da recomendação de corretivos e fertilizantes para a cultura da soja. *Rev. Bras. Ciência Solo* **2008**, *32*, 1661–1674. [CrossRef]
35. Murphy, J.; Riley, J.P. A modified single solution method for the determination of phosphate in natural waters. *Anal. Chim. Acta* **1962**, *27*, 31–36. [CrossRef]
36. MclNTOSH, J.J.; COX, J.E. Colorimetric Determination of Boron in Porcelain Enamel Frits. *J. Am. Ceram. Soc.* **1960**, *43*, 123–124. [CrossRef]
37. Luengo, R.F.A.; Calbo, A.G.; Lana, M.M.; Moretti, C.L.; Henz, G.P. *Classificação de Hortaliças*; Ministério da Agricultura, Pecuária e Abastecimento: Marília, Brazil, 1999; p. 63.
38. Epagri. Empresa de Pesquisa Agropecuária e Extensão Rural de Santa. In *Banco de Dados de Variáveis Ambientais de Santa Catarina*; Epagri: Florianopolis, Brazil, 2020; ISBN 2674-9521.
39. Agriculture and Agri-Food Canada. *Government of Canada Cool Wave Days for Cool Season/Overwintering Crops (>5 °C)*; Agriculture and Agri-Food Canada: Ottawa, ON, Canada, 2018.
40. Tremblay, N.; Bouroubi, Y.M.; Bélec, C.; Mullen, R.W.; Kitchen, N.R.; Thomason, W.E.; Ebelhar, S.; Mengel, D.B.; Raun, W.R.; Francis, D.D.; et al. Corn Response to Nitrogen is Influenced by Soil Texture and Weather. *Agron. J.* **2012**, *104*, 1658–1671. [CrossRef]
41. Parent, L.E.; Dafir, M. A Theoretical Concept of Compositional Nutrient Diagnosis. *J. Am. Soc. Hortic. Sci.* **1992**, *117*, 239–242. [CrossRef]
42. Rozane, D.E.; Vahl de Paula, B.; Wellington Bastos de Melo, G.; Haitzmann dos Santos, E.M.; Trentin, E.; Marchezan, C.; Stefanello da Silva, L.O.; Tassinari, A.; Dotto, L.; Nunes de Oliveira, F.; et al. Compositional Nutrient Diagnosis (CND) Applied to Grapevines Grown in Subtropical Climate Region. *Horticulturae* **2020**, *6*, 56. [CrossRef]
43. Montañés, L.; Heras, L.; Abadía, J.; Sanz, M. Plant analysis interpretation based on a new index: Deviation from optimum percentage (DOP). *J. Plant Nutr.* **1993**, *16*, 1289–1308. [CrossRef]

44. CQFS-RS/SC. *Manual de Calagem e Adubação para os estados do Rio Grande so Sul e Santa Catarina; Sociedade Brasileira de Ciência do Solo/Núcleo Regional Sul*, 11th ed.; Westphalen, F., Ed.; Sociedade Brasileira de Ciência do Solo: Viçosa, Brazil, 2016; ISBN 978-85-66301-80-9.
45. Barber, S. *Soil Nutrient Bioavailability. A Mechanistic Approach*, 2nd ed.; Wiley: New York, NY, USA, 1995.
46. Bray, R.H. Confirmation of the nutrient mobility concept of soil-plant relationships. *Soil Sci.* **1963**, *95*, 124–130. [CrossRef]
47. Nowaki, R.H.D.; Parent, S.-É.; Cecílio Filho, A.B.; Rozane, D.E.; Meneses, N.B.; dos Santos da Silva, J.A.; Natale, W.; Parent, L.E. Phosphorus Over-Fertilization and Nutrient Misbalance of Irrigated Tomato Crops in Brazil. *Front. Plant Sci.* **2017**, *8*, 825. [CrossRef]
48. Lemaire, G.; Salette, J.; Sigogne, M.; Terrasson, J.-P. Relation entre dynamique de croissance et dynamique de prélèvement d'azote pour un peuplement de graminées fourragères. I.—Etude de l'effet du milieu. *Agronomie* **1984**, *4*, 423–430. [CrossRef]
49. Andrews, M.; Sprent, J.I.; Raven, J.A.; Eady, P.E. Relationships between shoot to root ratio, growth and leaf soluble protein concentration of Pisum sativum, Phaseolus vulgaris and Triticum aestivum under different nutrient deficiencies. *Plant Cell Environ.* **1999**, *22*, 949–958. [CrossRef]
50. Bradshaw, A.D. *Evolutionary Significance of Phenotypic Plasticity in Plants*; Dunlap, J.C., Friedmann, T., Goodwin, S.F., Eds.; Academic Press: Cambridge, MA, USA, 1965; Volume 13, pp. 115–155. ISBN 0065-2660.
51. Wit, C.T. de Resource use efficiency in agriculture. *Agric. Syst.* **1992**, *40*, 125–151. [CrossRef]
52. Beaufils, E.R. Physiological diagnosis: A guide for improving maize production based on principles developed for rubber trees. *Fertil. Soc. South Afr. J.* **1971**, *1*, 1–28.
53. Courbet, G.; Gallardo, K.; Vigani, G.; Brunel-Muguet, S.; Trouverie, J.; Salon, C.; Ourry, A. Disentangling the complexity and diversity of crosstalk between sulfur and other mineral nutrients in cultivated plants. *J. Exp. Bot.* **2019**, *70*, 4183–4196. [CrossRef]
54. Jeanne, T.; Parent, S.-É.; Hogue, R. Using a soil bacterial species balance index to estimate potato crop productivity. *PLoS ONE* **2019**, *14*, e0214089. [CrossRef]